Earth and Planetary Science Letters, 117 (1993) 235–250
Elsevier Science Publishers B.V., Amsterdam

[PT]

A paleomagnetic and geochemical record of the upper Cochiti reversal and two subsequent precessional cycles from Southern Sicily (Italy)

A.A.M van Hoof [a], B.J.H. van Os [b], J.G. Rademakers [a], C.G. Langereis [a] and G.J. de Lange [b]

[a] *Paleomagnetic Laboratory, Fort Hoofddijk, Budapestlaan 17, 3584 CD Utrecht, The Netherlands*
[b] *Institute of Earth Sciences, Department of Geochemistry, Budapestlaan 4, 3584 CD Utrecht, The Netherlands*

Received July 1, 1992; revision accepted March 3, 1993

ABSTRACT

A detailed paleomagnetic and geochemical study of the upper Cochiti (N-R) reversal recorded in marine marls on southern Sicily shows two consecutive and very rapid transitions (R-N and N-R) that coincide with distinct lithological boundaries. A 'Fe-migration model' is presented in which magnetite is formed under different diagenetic conditions. During sulphate reduction, originally formed ('primary') magnetite is preserved. This primary magnetite has recorded the pre-transitional normal polarity. After burial, migration of ferrous iron occurs and subsequent oxidation produces 'secondary magnetite', which records the post-transitional reversed polarity and produces the two apparent transitions. In addition, low temperature (LT) and high temperature (HT) components record the reversal in a slightly different way: the HT component being acquired with a delay. It is probable that both components reside in magnetite but have a different origin and grain size distribution, giving different blocking temperature spectra. The actual upper Cochiti reversal occurs at a level with an estimated astronomically calibrated age of 4.165 Ma.

1. Introduction

In recent years, an increasing number of detailed records of geomagnetic polarity reversals have been published and they have provided important information on the characteristics of polarity reversals. The majority of these records have been obtained from sedimentary sequences. This is because of their abundance relative to lava sequences and the fact that the time control is more favourable and the geomagnetic signal has registered continuously. There is, however, reason for considerable caution in interpreting reversal records from relatively slowly deposited sediments. This is not only because of evidence from volcanic records, which often show quite different transitional field behaviour, but also because many aspects of the mechanism of remanence acquisition in sediments are still poorly known. Indeed, it has recently been shown that a high temperature magnetite component (in two examples of marine sedimentary reversal records from Sicily) has a delayed remanence acquisition with respect to a low temperature component and probably does not reflect the true geomagnetic field during the reversal [1]. The magnetic minerals are unlikely to be detrital because the changes in direction take place at distinct lithological boundaries in the sediment. Hence, the mechanism for the delay suggested by Tucker [2,3] is invalid in the sediments under study. Van Hoof and Langereis [1] have suggested that the magnetic minerals carrying the components were authigenically formed under different and cyclically fluctuating paleo-redox conditions. It is likely that early diagenetic processes played an important role in the complex acquisition of remanence mechanism.

To contribute to our understanding of this mechanism, additional and detailed rock mag-

Fig. 1. Location of the Punta di Maiata section in Southern Sicily (Italy).

netic and geochemical investigations are clearly needed. To this end, the study of reversal records is particularly useful because the (rapid) change in the geomagnetic field to an opposite polarity provides an opportunity for obtaining temporal constraints on the delay of the remanence acquisition. Our current research concerns the reversals records (from the lower Thvera to the Gauss/Matuyama boundary) which are located in the Rossello composite section. This section consists of the marine marls from the Trubi and the Narbone Formation [4,5]. These sediments show a distinct cyclicity in both $CaCO_3$ content and weathering (induration) profile, a cyclicity which is related to the precessional cycle of the Earth's orbit [4,6].

In this paper, we present the paleomagnetic, rock magnetic and geochemical results of the upper Cochiti (UC) polarity reversal, sampled in the Punta di Maiata section, southern Sicily (Fig. 1). In addition, we sampled two subsequent precessional cycles in order to investigate the magnetic and geochemical changes due to a cyclically changing environment outside the transition. Finally, since the remanence is not simply of detrital origin, we introduce a model that accounts for the acquisition of the remanence during early diagenesis. In this model the changes in the directions of the remanence are thought to be caused by changes in paleoredox conditions in the sediment, as derived from the geochemical and rock magnetic data.

2. Geological setting and sampling

Punta di Maiata is a small, prominent cape in a series of cliffs along the south coast of Sicily (Fig. 1). The Punta di Maiata section forms the middle part of the Rossello composite section [4,5] and consists of marine marls of the Pliocene Trubi Formation; the bedding plane has a strike of 354°N and a dip of 13°E. The average sedimentation rate in this section can be determined accurately and proves to be remarkably constant: 4.5–5.5 cm/ky. The Trubi marls consist mainly of carbonates (60–80% $CaCO_3$) and a mixture of clay minerals, and they show a pronounced rhythmic bedding, which is characteristic for this formation on Sicily (Fig. 2). Small-scale sedimentary cycles are quadripartite and show a distinct grey–white$_{(1)}$–beige–white$_{(2)}$ colour layering [4]. The average thickness of these cycles (in which the grey and beige marls represent the less indurated, $CaCO_3$-poor beds) is approximately 1 m. The (midpoints of) individual grey layers have

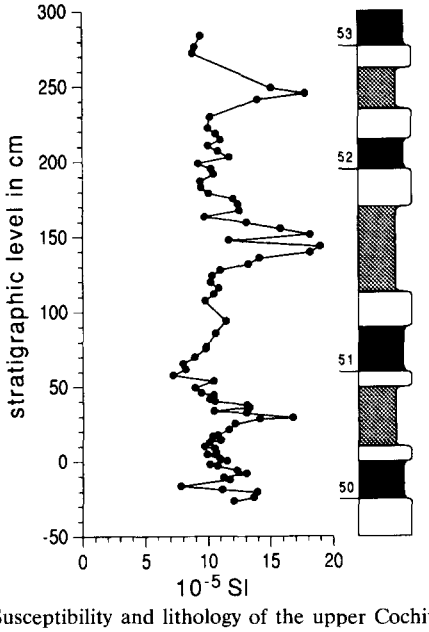

Fig. 2. Susceptibility and lithology of the upper Cochiti (UC) record. Small-scale sedimentary cycles are quadripartite and each comprises grey (shown as black)–white (white)–beige (shaded)–white (white) coloured marls. Cycle numbers are according to Hilgen (1987; 1991) and are shown to the left of the grey layer. Clear maxima of susceptibility are found in the beige layers, probably due to the higher clay content and the corresponding higher paramagnetic contribution.

been correlated to individual minima in the precession index [7], providing a high resolution astronomical polarity time scale [8]. Larger scale sedimentary cycles can be distinguished on the basis of the cyclic recurrence of relatively thick and/or indurated marly intervals in the succession [4,6]; they can be correlated to the eccentricity cycle with periods of 100 and 400 ky [8]. Although the weathering profile shows quite sharp changes in colour and induration, the changes in the fresh, unweathered sediment are much more gradual. The bottom part of the white$_{(1)}$ layers often shows brown oxidation spots, even in the freshest possible marls. These spots appear to be important with respect to both paleomagnetic and geochemical properties, as will be discussed later.

The samples were taken on the basis of the magnetostratigraphy of the Punta di Maiata section [5]. The section contains the upper Sidufjall reversal boundary, the Nunivak and Cochiti subchronozones and the Gilbert-Gauss reversal boundary. The stratigraphic interval in which the original upper Cochiti reversal was found was sampled in detail over a stratigraphic length of 120 cm. The two additional quadruplets were sampled over an interval of 220 cm. The record comprises the complete cycles 50, 51 and 52 (Fig. 2) [8]. The 0 level was defined at the boundary between the grey layer and the first white layer of cycle 50 (Fig. 2). Hence, the entire stratigraphic interval sampled ranges from -40 to 80 cm for the upper Cochiti reversal record, and from 80 to 300 cm for the two additional quadruplets. Due to the topography of the chosen sampling locality it was not possible to take samples below -40 cm. Furthermore, the lowermost part (-40–0 cm) consisted of fresh and clearly unweathered sediment but (despite our efforts to remove the weathered surface) in the middle and upper part the sampling of slightly weathered intervals could not always be avoided. The sediment particularly kept its weathering colour in the white layers (with the exception of white$_{(2)}$ of cycle 49); whereas in the beige layers the original light blue colour of the marls could usually be reached.

Sampling was carried out by taking oriented cores, 25 mm in diameter, approximately parallel to the bedding plane, at very close intervals (< 1 cm) from a freshly cut, near-vertical plane. In the laboratory, cores were cut into standard specimens 22 mm in height. The stratigraphic position of each specimen was accurately determined by taking into account the drilling orientation, strike and dip of the bedding plane and width of the saw cut.

For geochemical studies, the samples were cleaned by carefully scraping about 1 mm from the surface, followed by grinding and homogenising the sample in an agate mortar. For determination of major and trace element concentrations, a 250 mg portion of each sample was digested in a $HCLO_4/HF/HNO_3$ mixture. After digestion, the final solutions were made up in 50 ml 1 N HCl. Analyses of the total element concentrations of Al, Ti, Mn, Ca, S, Zr and Fe were made with an ARL34000 ICP emission spectrometer. Carbonate content was calculated from the total Ca concentrations, with a correction of 2% for non-carbonate Ca: $CaCO_3 = (Ca_{total} - 2) \times 2.5$. The accuracy and precision of the analysis was monitored by replicate analyses of international and laboratory standards and was found to be better than 2% for the major elements Al, Fe, Al, Mn and Ca, and better than 3% for the elements S, Zr and Ti.

3. Rock magnetic and chemical properties

The cyclicity in the Trubi marls is related to the precessional cycle which causes changes in climate (by variations in seasonal contrasts) and thus in the concentration and nature of terrigenous (clay and other minerals) and biogenic (carbonate) material supplied to the sea bed. The rock magnetism of the Trubi marls in general has been studied extensively by van Velzen and Zijderveld [9,10]. They found magnetites to be the most important carrier of the natural remanent magnetisation (NRM). Small amounts of hematite may be present but it is unlikely that this mineral contributes to the remanence. In addition, some goethite is found in these sediments [9–11]. In order to distinguish magnetic changes caused by geomagnetic variations from those caused by lithological variations and early diagenetic processes, a number of geochemical and rock magnetic properties of the sediment were determined. The rock magnetic properties concern the initial susceptibility (X_o), remanent saturation

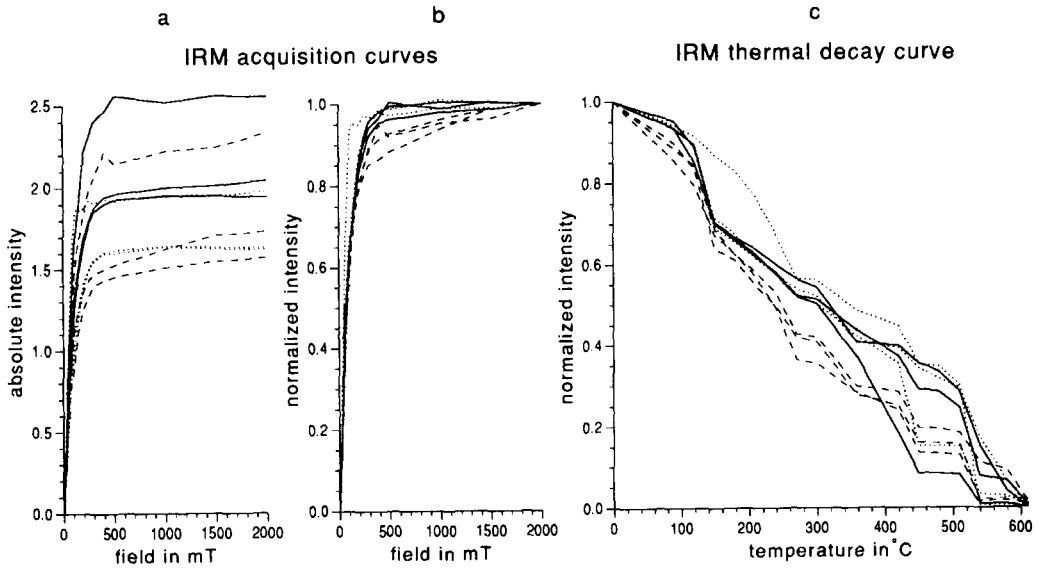

Fig. 3. (a) and (b) IRM acquisition curves and (c) subsequent thermal demagnetization of the saturation IRM for various lithologies from the UC reversal record. Grey, white and beige layers are denoted by solid, dotted and dashed lines, respectively. Grey and white layers (almost) reach saturation at 200–300 mT, whereas beige layers are not even totally saturated in the highest fields.

magnetisation (J_{rs}), the remanent coercive force (H_{cr}) and their interparametric ratios.

3.1. Rock magnetic results

X_o is strongly concentration dependent, and it also depends on the grain size and type of magnetic mineral. The X_o of the three precessional cycles (Fig. 2) is not significantly higher in grey than in white, but it shows prominent maxima in the beige layers.

IRM acquisition curves of a number of samples from different lithologies in the UC reversal were determined (Fig. 3a,b). Samples from the

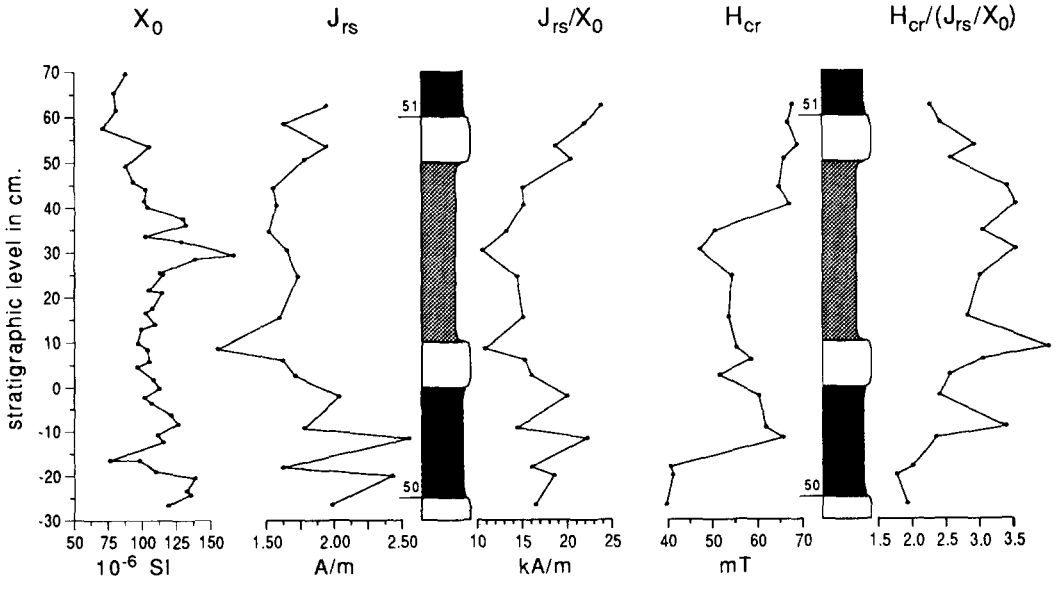

Fig. 4. Rock magnetic properties for the UC reversal record, involving susceptibility, X_o, saturation remanence J_{rs}, their ratio, X_o/J_{rs}, the remanent coercive force, H_{cr}, and their interparametric ratio $H_{cr}/(J_{rs}/X_o)$. See text for further discussion.

white and grey layers are almost saturated (92–96%) after application of a 300 mT field, and are fully saturated after application of a 400–500 mT field. Samples from the beige layers are only saturated after application of the highest fields (1.5–2.0 T) because of the presence of some additional high coercivity mineral, such as goethite or hematite. Subsequent thermal demagnetisation of the J_{rs} (Fig. 3c) does support the presence of some goethite in the beige layer: the decay of the saturation remanence at 100–120°C (the maximum unblocking temperature of goethite) is slightly larger for the beige layers than for the grey and white layers. More significant, however, is the decrease in the intensity at 135–155°C, which is probably caused by the reduction of stress in superficially maghemitised single domain magnetite grains [10]. The observed maximum blocking temperatures support the presence of magnetite as the dominant magnetic mineral.

The J_{rs} decreases with increasing grain size but (like the susceptibility) is not a good grain size indicator since it depends mainly on the concentration and type of the magnetic material. The J_{rs}/X_o ratio, however, may eliminate the dependence of J_{rs} and X_o on concentration (if only one magnetic mineral is dominant). In the case of magnetite, the ratio increases with decreasing grain size. The J_{rs}/X_o values in the grey and white layers (15–25 kA/m; Fig. 4) support the idea that magnetite is the dominant magnetic mineral but the ratio is lower in the beige layer (10–15 kA/m).

The remanent coercive force H_{cr} is largely independent of the concentration of magnetic material and can, therefore, be used to discriminate between different magnetic minerals. H_{cr} values are generally 50–70 mT, which is somewhat high for fine grained magnetite [12,13]. The H_{cr} values are significantly lower for stratigraphic levels between −30 and −15 cm; that is, in white$_{(2)}$ and the lower part of the grey layer, and highest from −10 to 0 and from 40 to 60 cm. H_{cr} values tend to increase if some weathering has occurred, which may explain the higher values between 40 and 60 cm, but this cannot explain the high values in the upper part of the grey layer, which showed very fresh sediment during

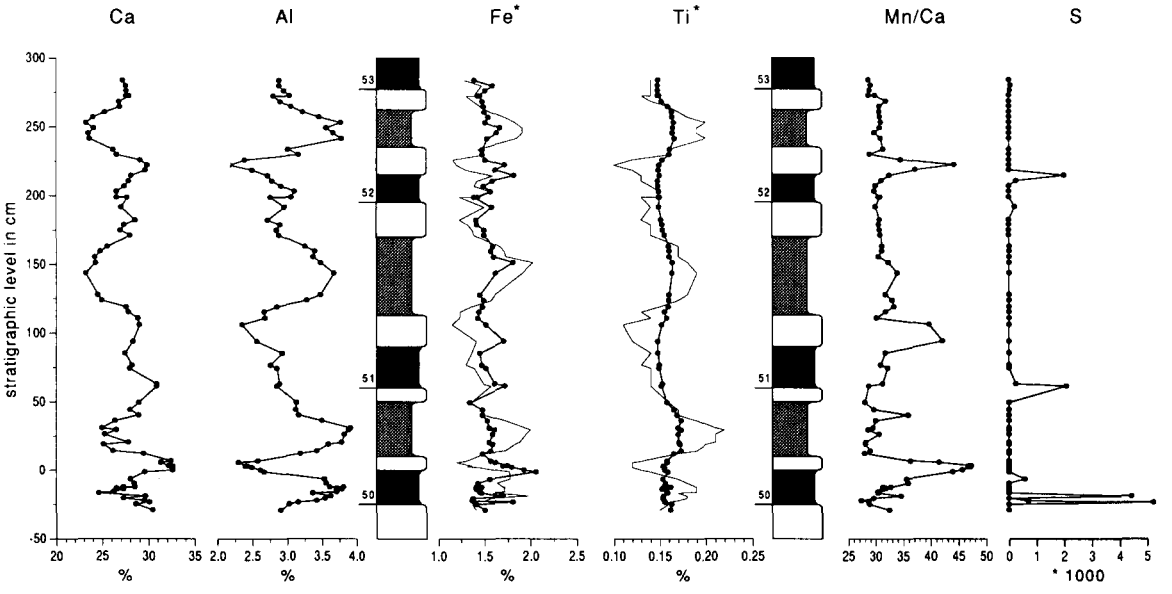

Fig. 5. Abundances of the most relevant elements: Ca, Al, Fe (thin line), Fe* (Fe/Al, thick line), Ti (thin line), Ti* (Ti/Al, thick line), Mn/Ca and S. The high calcium carbonate content causes the concentrations of all major elements to show a negative relation with Ca concentrations (closure effect). We have assumed a more-or-less constant non-carbonate input, as is suggested by rather constant Zr/Al and Ti/Al ratios (although the Ti/Al ratio seems to be slightly higher in the beige layers). The grey layers show some sulphur (*S*) spikes (0.2–0.5%), everywhere else the concentration of sulphur is below the detection limit.

sampling. Further, the relatively low H_{cr} values in the beige layer give no clear indication of a high coercivity mineral, as could be deduced from the IRM acquisition curves (Fig. 3). Apparently, the contribution of magnetite (85–95%, Fig. 3) strongly dominates the remanent coercive force.

The $H_{cr}/(J_{rs}/X_o)$ ratio may give useful information on both magnetic mineralogy and grain size. The values for this ratio (generally 2–2.5, but > 3 in beige) are somewhat high for fine-grained magnetites. The deflection of the $H_{cr}/(J_{rs}/X_o)$ and the J_{rs}/X_o ratios from the values for fine-grained magnetites is probably not due to a significant change in magnetic minerals, but rather to a change in the concentration of clay minerals. The paramagnetic contribution of the clay minerals in X_o is some tens of percent and shows maxima in the beige layers [11]. A correction for this paramagnetic contribution of the $H_{cr}/(J_{rs}/X_o)$ and the J_{rs}/X_o values will change these ratios into values more (but not entirely) compatible with fine-grained magnetites. It is probable that changes in magnetomineralogy occur that are related to the different (beige) lithology, but these changes remain largely unnoticed due to the dominance of the paramagnetism.

3.2. Geochemical results

Relatively high concentrations of carbonate (65–70%) are found in the white layers, intermediate values in the grey layers (60–65%) and low values in the beige layers (55%) (Fig. 5). The white$_{(1)}$ beds have slightly higher carbonate values than the white$_{(2)}$ layers. Mainly due to the high calcium carbonate content of the sediment, the concentrations of all major elements show a negative relation with Ca concentrations (closure effect) (Fig. 5). We have assumed a more-or-less constant non-carbonate input, as is suggested by rather constant Zr/Al and Ti/Al ratios; although the Ti/Al ratio does seem to be slightly higher in the beige layers (Fig. 5). Therefore, all concentrations were divided by the Al content of the samples, in order to compensate for carbonate dilution.

The grey layers show some sulphur spikes of 0.2–0.5% (Fig. 5), and some sulphur is found in the lowermost part of the record. Everywhere else, the concentration of sulphur is below the detection limit. Although some weathering has occurred, these sulphur enrichments are probably relict iron sulphides, as is indicated by coinciding iron peaks: iron sulphides are authigenically formed during sulphate reduction shortly after deposition [14]. The highest sulphur content is found in the grey layer of cycle 50 (0.5%). This suggests that within this cycle the diagenetic conditions were the most reducing during the formation of the grey layer, rather than during the formation of the white and beige layers. The same may apply to the grey layers of other cycles. The increased subaerial weathering in the middle and upper part of the record observed during sampling, however, very likely resulted in the oxidation of most sulphides in the grey layers of cycles 51 and 52, causing the lower sulphur concentrations.

Manganese is a good indicator for paleoredox conditions [15]. Manganese concentrations are generally low and display values of 600–800 ppm in the grey and beige layers (which have a low to moderate carbonate content), but may go up to 1600 ppm in the carbonate-rich white$_{(1)}$ layers. The general distribution of Mn seems closely related to the carbonate content and may well be determined by manganese adsorption and subsequent overgrowth on calcite surfaces [16–18]. This correlation is clearly demonstrated by the relatively constant Mn/Ca ratio, but the white$_{(1)}$ layers display a large enrichment of Mn over Ca. The higher Mn/Ca ratio in the white$_{(1)}$ layers compared with the white$_{(2)}$ layers (Fig. 5) suggests that more dissolved manganese was available during or after the formation of the white$_{(1)}$ layers.

The organic carbon content has not been measured in these samples. In a series of quadruplets from the same Punta Maiata section, values were found to vary between 0.05% and 0.25% [19]. The organic carbon content is highest in the grey, intermediate in the white and lowest in the beige layers. At younger stratigraphic levels in the Trubi Formation, the grey layers are laminated and they are often developed into diatomitic or sapropelitic layers [4], typical of a higher organic carbon content.

The differences in lithology (and thus in the chemical composition and magnetic mineral content of each layer) are reflected in the geochemical and rock magnetic parameters. The initial

susceptibility values are higher in the beige layers, which can be explained by the higher concentrations of Fe and, possibly, higher concentrations of Ti (Figs. 4 and 5). The higher Fe content (even when corrected for Al) may be caused by an increase of (Fe-containing) clay minerals, rather than by a higher concentration of (ferri)-magnetic minerals [20]. Similarly, the higher Ti concentration may reside in titanium magnetites (or titanium maghemites), which also causes a higher susceptibility, although no clear evidence for titanium magnetites is provided by the rock magnetic properties. Any existing titanium magnetites may be masked, however, and not contribute to the remanence: coarse-grained titanium magnetite was found in the magnetic concentrates of the Calabrian (southern Italy) Trubi Formation and was shown not to carry any noticeable remanence [21]. In addition, other mineral phases, such as rutile and ilmenite, dominate the Ti concentration.

This enrichment in iron-rich minerals strongly influences the rock magnetic properties, which are directly related to the concentration of magnetic minerals, like X_0 and J_{rs}. It should further be realised that these properties, although showing a linear relation with concentration, are also influenced by changes in grain size and the crystallinity of the magnetic minerals.

4. NRM components

4.1. Demagnetisation

Thermal demagnetisation of the natural remanent magnetisation (Fig. 6) generally shows the presence of three components, as usually found in these Trubi marls [5,11]. Apart from a small laboratory-induced component removed at 90–100°C (which had an orientation related to storage), there is often a first component that has the present field direction and is removed at 200–250°C. It is clearly of secondary origin and must be due to weathering, since this component does not occur in the lowermost and least weathered part of the record (Fig. 6a).

A characteristic remanence is generally removed at higher temperatures and consists of two components. A low temperature (LT) component is removed between 250°C and 360–450°C. In some samples, the direction of the remanence starts to fluctuate at temperatures higher than 390°C (Fig. 6h). These fluctuations are due to viscous behaviour, probably caused by the production of superparamagnetic magnetite grains during heating, due to the oxidation of pyrite [10]. Although in most of the record sulphur is below the detection limit, trace amounts of pyrite are probably sufficient to produce a (magnetically) detectable amount of magnetite. A high temperature (HT) phase is usually removed at 580°C and occasionally at somewhat higher temperatures (610°C). The HT component is most probably carried by single domain magnetite [9]. The LT and HT components have both been determined for every sample, where possible. Poorly determined directions, resulting from very low intensities and/or scatter, have not been plotted in Fig. 8.

The demagnetisation diagrams further show the same clockwise rotation as observed in the other Trubi sections on Sicily [5,22]. The characteristic remanence directions are marked by consistently shallower inclinations than the geocentric axial dipole field for southern Sicily, which is probably due to sediment compaction [23,24].

Blocking temperature spectra for the different lithologies have been determined throughout the section (Fig. 7). They show a similar trend for all

TABLE 1

The mean directions for the reversed and normal intervals

		N	Declination	Inclination	α_{95}	R_{sum}
Reversed	below −27.5 cm	7	214.1°	−39.2°	9.8	6.847
Normal	−24.1 to −4.4 cm	31	29.7°	54.8°	3.9	30.591
Reversed	above 26.3 cm	78	213.8°	−41.3°	2.3	76.382

N = the number of samples.
α_{95} = the cone of confidence at the 95% level.
R_{sum} = the vectorial sum of N unit vectors.

lithologies, in that the NRM decreases most rapidly between 510° and 600°C. The decay curves clearly indicate the presence of magnetite. Since the maximum unblocking temperatures are higher than 580°C [21,25,26], this magnetite is probably slightly cation deficient. In general, the beige layers show appreciably lower NRM intensities, which is in agreement with the rock magnetic and geochemical data.

4.2. *The reversal record*

The directions of the LT and HT components for the upper Cochiti record are shown in Fig. 8.

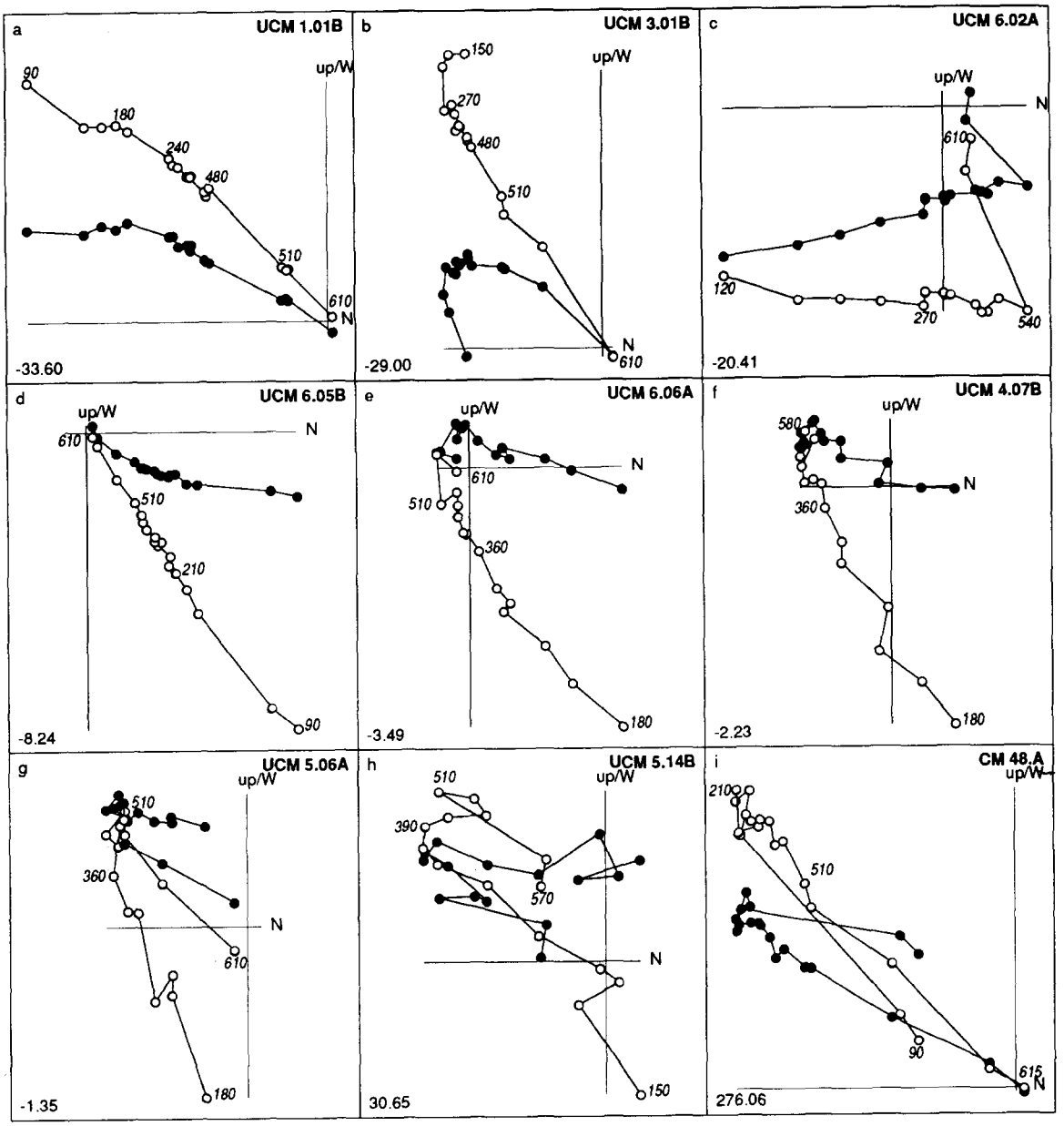

Fig. 6. Thermal (th) demagnetization diagrams of nine representative samples from the UC reversal and the two additional quadruplets. Outlined symbols = projection on the vertical plane; black symbols = projection on the horizontal plane; the stratigraphic level is plotted in centimetres in the bottom left-hand corner; numbers refer to temperatures in degrees Centigrade; *tc* = tilt correction has been applied.

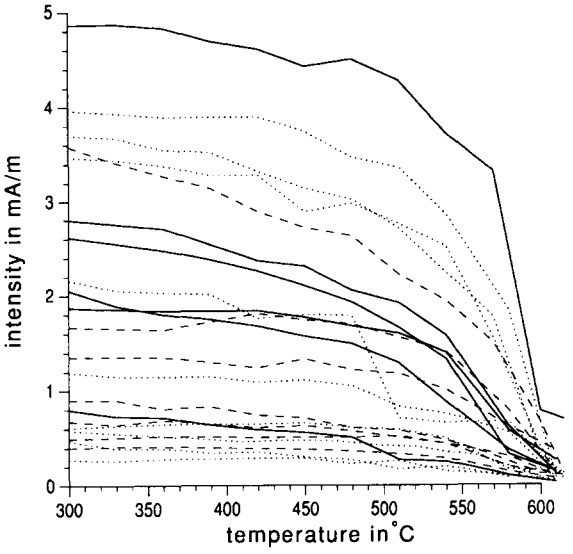

Fig. 7. The NRM decay curves (starting at 300°C) of beige (dashed lines), white (dotted lines) and grey (solid lines) marl samples. Intensities are generally lower for the beige marls than for the grey and white marls. Maximum blocking temperatures are indicative of (cation deficient) magnetite.

For the earlier magnetostratigraphic study of the Punta di Maiata section [5], most samples were taken in the grey and beige layers. The reversal was, therefore, thought to occur between the grey and beige layer of cycle 50. It now appears, however, to be a more complex reversal showing reversed directions in the white$_{(2)}$ layer of cycle 49. The mean directions for the reversed and normal intervals are given in Table 1. The mean declinations are essentially the same as the general 35° clockwise rotation of the Caltanisetta basin [22].

The first (R-N) transition is characterised by an instantaneous polarity change of the HT component at −25 cm, at the boundary of white$_{(2)}$ to grey, with no (reliable) intermediate directions. The LT component shows a similarly quick change in declination, whereas its inclination seems to reverse more gradually. Clearly, the LT reversal takes place at a somewhat higher level (−25– − 15 cm). The HT polarities remain normal in the interval from −25 to −5 cm, and the average declination is only slightly less than the generally observed 35°, but inclinations are a bit steeper than usual.

The second transition (N-R) is at the −5 cm level, just below the boundary of grey to white$_{(1)}$. The HT component again changes very rapidly from normal to reversed polarity with no interme-

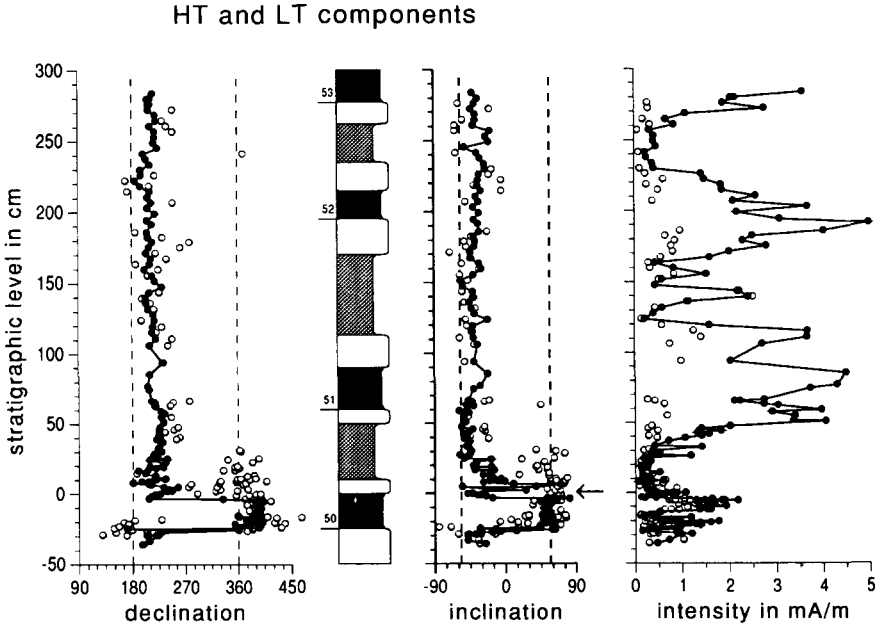

Fig. 8. LT (circles) and HT (dots) components of the UC reversal record and two subsequent precessional cycles, and their respective intensities. Diamonds = directions that could not reliably be interpreted due to very low intensities, random scatter and/or significant viscous behaviour at higher temperatures; arrow indicates where the maximum in Mn was found.

diate directions. After this sharp transition, the HT component shows a 'normal excursion', especially in inclination. Alternatively, one could interpret the sudden change to reversed polarity as a short 'reversed excursion' (between −5 and 5 cm), only just before a more gradual change from normal to reversed, say from 5 to 15 cm. Remarkably, this 'reversed excursion' coincides exactly with the peak in Fe* and Mn/Ca (Fig. 5); the latter ratio is a good paleoredox indicator, as mentioned above.

The LT component changes polarity at distinctly higher levels, approximately between 30 and 35 cm, and coinciding with a relatively small but significant peak in Mn/Ca (Fig. 5). The relatively small directional changes in the HT component above 26 cm are compatible with secular variation changes smoothed by sedimentary remanence acquisition and are similar to those observed in the upper Kaena reversal record [20].

5. Discussion

The initial location of the reversal was based on the magnetostratigraphy of the Punta di Maiata section [5], for which samples were taken mainly from the grey and beige layers. Hence, the reversed polarities in white$_{(2)}$ of cycle 49 were then not found. Since the beige layer of cycle 49 shows normal polarities [5], this implies that there must be yet another (N-R) transition, recorded somewhere near the transition of beige to white$_{(2)}$ in cycle 49.

It is clear that the transitions recorded are not caused by a rebound or excursion related to the UC reversal, but are more probably caused by early diagenetic conditions that vary with the lithology. Therefore, interpretation in terms of timing and duration of the two recorded transitions (while a third transition must occur below) is not meaningful. Early diagenetic changes cause one and the same reversal to be recorded several times, via a delayed acquisition mechanism [1]. In addition, the coincidence of two extremely rapid reversals that occur exactly at distinct lithological or geochemical boundaries (apparently related to paleoredox boundaries) makes any interpretation in terms of geomagnetic field behaviour improbable. The assertion that sediments have a resolution determined by the most rapid changes recorded [27] is, therefore, not generally valid, even though the sediment may have no visible (lithological) boundaries. We thus emphasise the need for additional and detailed lithological (and rock magnetic and geochemical) information on reversal records. Due to the very rapid changes in the magnetic remanence, no intermediate directions were recorded and we therefore refrain from presenting VGP paths. It is more useful to discuss the paleoredox conditions and corresponding diagenetic changes that may have caused the observations.

5.1. Diagenetic changes during deposition

The alternating sequence of beige (carbonate poor with iron (hydro)oxides), white (carbonate rich) and grey layers (richer in organic matter than beige and white and containing sulphides, Fig. 5) suggests that the diagenetic conditions changed from oxic via suboxic to anoxic for the respective layers [28,29]. The differences in diagenetic stages are caused by different amounts of reactive organic matter in each layer; that is, a higher amount of organic matter will lead to an enhanced consumption of oxidants used for the degradation of organic matter. After oxygen is depleted, nitrate, manganese oxides, iron hydroxides and finally sulphate will be used as electron acceptors [29,30].

Bacterially mediated magnetite formation has been reported to occur under oxic and suboxic conditions [31], whereas anoxic conditions inhibit bacterially mediated magnetite formation, due to competition in the substrate with sulphate-reducing bacteria. This implies that, during the deposition of the white and beige layers, magnetite formation continued, while during the deposition of the grey layer magnetite formation was inhibited in the anoxic part of the sediment. The unlaminated appearance of the grey layer suggests that conditions were not fully anoxic during deposition. Therefore, sulphate reduction did not occur at the top of the sediment. Above the zone of sulphate reduction, iron hydroxides, manganese oxides, nitrate and even oxygen may have been used as oxidants for the decomposition of organic matter and thus suboxic conditions may have developed during the deposition of the grey

layer, causing the formation of magnetite (at time $t = 1$, Fig. 9).

During burial, magnetite dissolution may occur in the sulphate reduction zone [32]. However, because of the higher reactivity towards HS^- of dissolved iron, amorphous and poorly crystalline iron (such as lepidocrocite, goethite and hematite), magnetite may persist in this zone. Magnetite is only attacked after all other iron oxide phases are "titrated" with HS^- [33,34]. In addition, magnetite is resistant to microbial iron reduction [35,36]. Evidently, the IRM acquisition, as well as the IRM and NRM thermal decay curves imply the presence of magnetite and thus its preservation during sulphate reduction (Figs. 3 and 7).

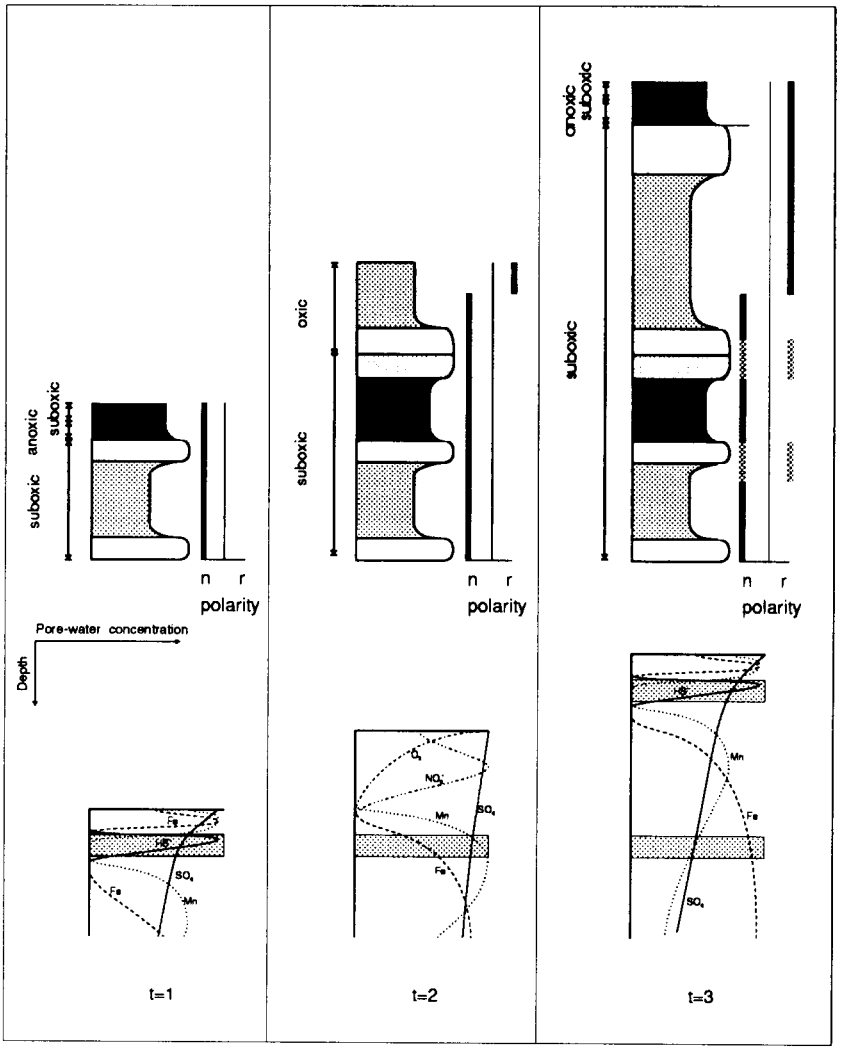

Fig. 9. The 'Fe-migration model' with the pore water concentrations plotted against depth at the time of deposition. During deposition of the anoxic grey layer 'primary' magnetite was formed at $t = 1$. During post-oxic diagenesis, upon burial by the white and beige layers, 'secondary' magnetite is formed by migration of Fe^{2+} (at $t = 2$ and $t = 3$). Primary magnetite causes the geomagnetic field to be recorded during or very shortly after the initial formation of this magnetite, by growing through its critical blocking diameter and causing acquisition of a CRM. Upon burial of the grey layer, secondary magnetite is formed on either side of the grey layer (in the white layers); in the grey layers this depends on the redox circumstances. If, at that moment, a polarity reversal occurs, the secondary magnetites will record the new polarity. The presence of already formed primary magnetite (which had recorded the old polarity) competes with the secondary magnetite (dashed polarities). If secondary magnetite predominates, the resulting direction will reflect the new polarity, in our case reversed. Lithology as in Fig. 2.

The magnetic minerals that could form during sulphate reduction are greigite and pyrrhotite [37]. However, greigite and pyrrhotite would normally not survive oxidation, because of subaerial weathering, for example. The formation of greigite and pyrrhotite has been reported to occur mainly in a low sulphate environment and thus they are mainly found in fresh and brackish water sediments [38]. Moreover, greigite and pyrrhotite are not found in recent anoxic basins [39,55]. Conclusively, chemical and rock magnetic results indicate that magnetite is the main carrier of the magnetic signal and that it is not significantly dissolved during sulphate reduction in these sediments.

5.2. *Processes after deposition*

Shortly after the deposition of a grey anaerobic layer (at time $t = 2$, Fig. 9), the organic carbon flux diminishes and sulphate reduction ceases. As a result, the dissolution of magnetite by HS^- will also stop. This situation will cause a surplus of oxygen over the reductive species in the subsequently deposited organic-poor beige and white layers. Reductive species in these layers (organic matter and possibly sulphides) will be oxidised and the oxidation front will move down relative to the sediment–water interface. This formation of a progressive oxidation front is similar to that described in the "burn-down" model developed by Wilson et al. [40] and is best marked by the redox-sensitive elements Fe and Mn. Diffusion of dissolved Fe and Mn from the reduced zone towards the oxygen boundary can cause the formation of iron and manganese enrichments (amorphous Fe and Mn (hydr)oxides) at the top of the reduced layer [41–43]. The iron enrichments found above the grey layers in the bottom part of the white$_{(1)}$ layers (Fig. 5) are clearly the result of this process.

The oxidation front can only penetrate slowly into the grey layer because this contains high levels of organic carbon and of sulphides. In addition, the oxidation of pyrite by the Fe(III) iron still available in the grey layer will increase the upward flux of Fe^{2+}. This occurs following the reaction [44,45]:

$$FeS_2 + 14Fe^{3+} + 8H_2O \rightarrow 15Fe^{2+} + 2SO_4^{2-} + 16H^+ \quad (1)$$

This additional supply of reduced species will hamper the descent of the oxidation front and will enhance the iron enrichment at the top of the grey layer and in the superimposed white$_{(1)}$ layer.

5.3. *Processes after burial*

After deposition of the white and the beige layer on top of the grey layer, a new cycle begins with the deposition of a new white$_{(1)}$ and a grey layer (at time $t = 3$, Fig. 9). An increased flux of organic matter during the formation of the new grey layer will merely stop the downward diffusion of oxygen. Subsequently, below the newly deposited grey layer, oxygen will become rapidly exhausted. However, the low content of organic matter in the beige and white layers between the new and the buried grey layer will not support sulphate reduction. The diagenetic stage between sulphate and Mn reduction, coinciding with a low reactive organic carbon content, is called post-oxic, following the classification of Berner [39] and can be compared with suboxic conditions [30,40].

In the buried grey layer pyrite oxidation probably continues, although oxygen is exhausted. The remaining Fe(III) iron in this buried grey layer (iron hydroxides) enhances the oxidation of pyrite, providing a continuous source of Fe^{2+}.

Karlin [46] found that magnetite is formed under suboxic conditions between the nitrate and iron reduction zone. Bacterially mediated magnetite formation can occur under such conditions [36,47]. Dissimilatory iron-reducing micro-organisms can form magnetite provided that reactive Fe(III) iron is present [36]. Therefore, magnetite formation will be especially enhanced at the very reactive iron enrichment zone formed during burn-down just above the buried grey layer (the 'reversed excursion'; see section 4.2), but may also occur to a lesser extent just below the grey layer. The previously formed iron hydroxides are an ideal substrate on which dissimilatory micro-organisms can produce magnetite (Fig. 9, $t = 3$).

Within the buried grey layer itself, sulphate reduction and subsequent pyrite formation have diminished the amount of reactive iron available (see previous section). Obviously, magnetite for-

mation is not supported in the buried grey layer. Magnetite can precipitate directly in the surrounding white and beige layers following the reaction:

$$2Fe^{3+} + Fe^{2+} + 4H_2O \rightarrow Fe_3O_4 + 8H^+ \quad (2)$$

or via the bacterially mediated reaction:

$$CH_2O + 24Fe(OH)_3 \rightarrow 2CO_2 + 54H_2O + 8Fe_3O_4 \quad (3)$$

Magnetite formation takes place whenever the organic matter content and the dissolved oxygen concentration are low and Fe^{2+} and reactive iron oxides are available.

The preservation of magnetite is also enhanced by non-steady state (organic-rich versus organic-poor) diagenesis. As mentioned above, an increasing flux of organic carbon (i.e. deposition of a new grey layer) causes an upward shift in the redox front. Such a shift can occur more rapidly than iron and manganese oxides at the redox front may dissolve, thus allowing these oxides to survive [46]. Similarly, Finney et al. [15] found a correlation between the preservation of manganese oxide peaks and an increased organic carbon flux. However, persisting suboxic conditions will eventually dissolve all manganese oxides [43,48–50]. Not only the co-precipitation of Mn with calcite but also the adsorption/recrystallisation of Mn on calcite can induce the formation of Mn-enriched crusts [16,17]. As a consequence of this previously formed manganese hydroxides be preserved during suboxic diagenesis. The peaks in the Mn/Ca observed in the $white_{(1)}$ layers above the grey layers are the result of this process. The presence of Mn enrichments in carbonate-rich rocks can indicate a change in the environmental regime and thus the formation of magnetite during diagenesis. Straightforward evidence for the preservation of magnetite is given by the presence of the iron enrichments at the top of the grey layers, just below the Mn enrichments, as is shown by the Fe/Al ratios (Fig. 5). The -15 to $+15$ cm interval is a classical example of such a sequence of these redox-mobile elements, indicating their mobilisation in the grey layer followed by upward flux to the overlying white/beige layer [43]. The preservation of this diagenetic Fe layer and magnetite indicates that the redox conditions after the formation of this layer did not reach the iron reduction stage.

5.4. *Implications and conclusions*

From our discussion above it follows that magnetite can be formed in different stages of diagenesis: during deposition primary magnetite is formed (Fig. 9, $t = 1$) and during suboxic diagenesis secondary magnetite (Fig. 9; $t = 3$). Primary magnetite causes the geomagnetic field to be recorded during or very shortly after the initial formation of this magnetite, by growing through its critical blocking diameter and causing acquisition of a chemical remanent magnetisation (CRM). This process is very similar to that described earlier by Channell et al. [51] in Italian sections, where secondary hematite acquired a delayed remanence due to an authigenic CRM at some depth below the interface. The depth at which this occurs (presumably in the iron reduction zone) may vary with lithology, but is probably comparable with post-depositional remanent magnetisation (PDRM) lock-in depths (15–20 cm). In fact, magnetite grains acquiring a CRM will probably be subject to typical PDRM lock-in depth intervals where grains carrying CRM are mechanically fixed, mainly through compactional loading [52]. This would imply a minimum lock-in depth of approximately 15 cm. A maximum lock-in depth, however, depends on the depth of CRM acquisition, which may be well below maximum PDRM lock-in depths. Indeed, our recent work shows possible depths of as much as 80–120 cm [1,20].

Upon burial of the grey layer, secondary magnetite is formed on either side of the grey layer (in the white layers), depending on the amount of reactive iron. If at that moment a polarity reversal occurs, it will record the new polarity. The presence of already formed primary magnetite (bearing a record of the old polarity) competes with the secondary magnetite. If secondary magnetite predominates, the resulting direction will reflect the new polarity; in our case reversed. At the same time, intensities are much lower in the white layers (Fig. 8) as a consequence of the vectorial sum of both recorded opposite directions/polarities. Thus, besides a lower geomagnetic field intensity during a transition, the mech-

anism of opposite directions may also cause lowered NRM intensities.

There is an additional complication represented by the presence of both a LT and HT component. As observed earlier [1], there is a difference in acquisition between the two components: the HT component shows a delay with respect to the LT component. In other words, the LT component has already locked the old polarity (normal, e.g., between 0 and 25–30 cm), while the minerals carrying the HT component are still being formed and have not yet grown through their critical blocking diameter. However, the LT component itself also shows a delayed CRM acquisition, as evidenced by the reversed polarities in the lowermost part of the record (Fig. 8). Thus, the LT component may record the ambient polarity before the HT component, but it is also subject to a 'secondary' formation. Obviously, this yields some information on the magnetic minerals carrying the LT component.

Contrary to our earlier suggestions [1] we find it unlikely that the LT component is carried by pyrrhotite or some other magnetic iron sulphide. Firstly, the temperature trajectory that determines the LT component has much higher blocking temperatures than the Curie temperature of pyrrhotite ($\pm$320°C) [53]; sometimes it is only totally removed at temperatures of 510–540°C (Fig. 6). Secondly, detailed rock magnetic studies of the Trubi marls from Sicily have shown no evidence for pyrrhotite [9,10]. Also our present geochemical data and discussion above virtually exclude the existence of pyrrhotite. Therefore, we assume that the LT component also resides in magnetite. The different (and varying) blocking temperature spectra of the LT and HT components probably reflect different grain-size spectra that, in turn, reflect their (authigenic) origin and timing of formation. The earlier lock-in of the LT component argues for a larger grain size than that of the HT component; that is, the LT magnetite has grown through its critical blocking diameter before the HT magnetite. An alternative explanation for the lower blocking temperatures of the LT component (grain sizes near the threshold of single domain and superparamagnetic grains) is unlikely, since it would imply partial dissolution of the earlier locked-in LT magnetite and the simultaneous growth/formation of secondary (HT) magnetite. Some unexplained details in the record, such as the occurrence of reversed LT directions in the bottom part of the grey layer, leads us to suspect that the actual processes are even more complicated. Clearly, additional rock magnetic studies attacking this particular problem are needed.

The sequence of events suggested by our current 'Fe-migration model' (primary magnetite preserved in the grey layer and the formation of secondary magnetite especially in the white$_{(1)}$ layer) supplies us with a quite accurate location for the actual reversal. The grey layer of cycle 51 consistently shows reversed polarities, suggesting that, at least here, the geomagnetic transition has been completed. We retain, as our best and most consistent estimate, the level where both LT and HT directions consistently show a reversed polarity; that is, approximately at the 35 cm level.

In principle, this level gives a more accurate age than the one previously established, 4.18 Ma [8], on the basis of the initial magnetostratigraphy [5]. The 35 cm level gives an age of 4.165 Ma, taking into account a lag of 3–4 ky between precessional forcing and climate response [54].

Acknowledgements

Adry van Velzen was most helpful in the field. P. Anten carried out the geochemical analyses. C. Laj and an anonymous reviewer are thanked for their detailed criticism which led to a considerable improvement in the manuscript. The research was supported by the Netherlands Foundation for Earth Sciences (AWON) with financial aid from the Netherlands Organisation for Scientific Research (NWO).

References

1 A.A.M. van Hoof and C.G. Langereis, Reversal records in marine marls and delayed acquisition of remanent magnetisation, Nature 351, 223–225, 1991.
2 P. Tucker, Selective post-depositional realignment in a synthetic sediment, Phys. Earth Planet. Inter. 20, 11–14, 1979.
3 P. Tucker, Stirred remanent magnetization: A laboratory analogue of post-depositional realignment, J. Geophys. 48, 153–157, 1980.
4 F.J. Hilgen, Sedimentary rhythms and high-resolution chronostratigraphic correlations of the Mediterranean Pliocene, Newsl. Stratigr. 17, 109–127, 1987.

5 C.G. Langereis and F.J. Hilgen, The Rossello composite: A Mediterranean and global reference section for the Early to early Late Pliocene, Earth Planet. Sci. Lett. 104, 211–225, 1991.
6 F.J. Hilgen and C.G. Langereis, Periodicities of $CaCO_3$ cycles in the Pliocene of Sicily: discrepancies with the quasi-periods of the Earth's orbital cycles?, Terra Nova 1, 409–415, 1989.
7 A.L. Berger and M.F. Loutre, Onsolation values for the climate of the last 10 million years, Quat. Sci. Rev. 10, 297–317, 1991.
8 F.J. Hilgen, Extension of the astronomically calibrated (polarity) time scale to the Miocene–Pliocene boundary, Earth Planet. Sci. Lett. 107, 349–368, 1991.
9 A.J. van Velzen and J.D.A. Zijderveld, Rock magnetism of the early Pliocene Trubi formation (Sicily), Geophys. Res. Lett. 17, 791–794, 1990.
10 A.J. van Velzen and J.D.A. Zijderveld, A method to study alterations of magnetic minerals during thermal demagnetisation applied to a fine-grained marine marl (Trubi Formation, Sicily), Geophys. J. Int. 110, 79–90, 1992.
11 A.A.M. van Hoof, Geomagnetic polarity transitions of the Gilbert and Gauss Chrons recorded in marine marks from Sicily, Geol. Ultraiectina 100, 1993.
12 R.L. Hartstra, Grain-size dependence of initial susceptibility and saturation magnetisation-related parameters of four natural magnetites in the PSD–MD range, Geophys. J.R. Astron. Soc. 71, 477–495, 1982.
13 D.J. Dunlop, Hysteresis properties of magnetite and their dependence on particle size: a test of pseudosingle domain remanence model, J. Geophys. Res. 91, 9569–9584, 1986.
14 R.A. Berner, Sedimentary pyrite formation, Am. J. Sci. 268, 1–23, 1970.
15 B.P. Finney, M.W. Lyle and G.R. Heath, Sedimentation at MANOP site H (eastern equatorial Pacific) over the past 4000,000 years: climatically induced redox variations and their effects on transition metal cycling, Paleoceanography 3, 169–189, 1988.
16 E.D. Boyle, Manganese carbonate overgrowth on foraminifera tests, Geochim. Cosmochim. Acta 47, 1815–181, 1983.
17 J. Thomson, S. Colley, N.C. Higgs, D.J. Hydes, T.R.S. Wilson and J. Sørensen, Geochemical oxidation fronts in NE Atlantic distal turbidites and their effects in the sedimentary record, in: Geology and Geochemistry of Abyssal Plains, P.P.E. Weaver and J. Thomson, eds., Geol. Soc. London Spec. Publ. 31, 167–177, 1987.
18 J.J. Middelburg, G.J. de Lange and C.H. van der Weijden, Manganese solubility control in marine pore waters, Geochim. Cosmochim. Acta 51, 759–763, 1987.
19 J.P. de Visser, J.H. Ebbing, L. Gudjunsson, F.J. Hilgen, F.J. Jorissen, P.J.J.M. Verhallen and D. Zevenboom, The origin of rhythmic bedding in the Pliocene Trubi formation of Sicily, Southern Italy, Palaeogeogr. Palaeoclimatol. Palaeoecol. 69, 45–66, 1989.
20 A.A.M. van Hoof and C.G. Langereis, The upper Kaena sedimentary geomagnetic reversal record from southern Sicily, J. Geophys. Res. 97, 6941–6958, 1992.
21 J.H. Linssen, Properties of Pliocene sedimentary geomagnetic reversal records from the Mediterranean, Geol. Ultraiectina, 80, 1–232, 1991.
22 P.J.J. Scheepers and C.G. Langereis, Analysis of NRM directions from the Rossello composite: implications for the tectonic rotations of the Caltanissetta basin (Italy), Earth Planet. Sci. Lett., submitted, 1993.
23 C. Laj, M. Jamet, D. Sorel and J.P. Valente, First paleomagnetic results from Mio–Pliocene series of the Hellenic sedimentary arc, Tectonophysics 86, 45–67, 1982.
24 G.L. Anson and K.P. Kodama, Compaction-induced inclination shallowing of the post-depositional remanent magnetisation in a synthetic sediment, Geophys. J.R. Astron. Soc. 88, 673–692, 1987.
25 F. Heider and D.J. Dunlop, Two types of chemical remanent magnetization during oxidation of magnetite, Phys. Earth Planet. Inter. 46, 24–45, 1986.
26 J.H. Linssen, Preliminary results of a study of four successive sedimentary geomagnetic reversal records from the Mediterranean (Upper-Thvera, Lower and Upper-Siduf-jall, Lower Nunivak), Phys. Earth Planet. Inter. 52, 207–231, 1988.
27 C. Laj, S. Guitton, C. Kissel and A. Mazaud, Complex behaviour of the geomagnetic field during three succesive polarity reversals, 11–12 m.y. B.P.J. Geophys. Res. 93, 11655–11666, 1988.
28 M. Lyle, The brown–green color transition in marine sediments: a marker of the Fe(III)–Fe(II) redox boundary, Limnol. Oceanogr. 28, 1026–1033, 1983.
29 G.J. de Lange, Early diagenetic reactions in interbedded pealgic and turbiditic sediments in the Nares Abyssal Plain (western North Atlantic): consequences for the composition of sediment and interstitial water, Geochim. Cosmochim. Acta 50, 2543–2561, 1986.
30 P.N. Froelich, G.P. Klinkhammer, M.L. Bender, N.A. Luedtke, G.R. Heath, D. Cullen, P. Dauphin, D. Hammond, B. Hartman and V. Maynard, Early oxidation of organic matter in pelagic sediments of the eastern equatorial Atlantic: suboxic diagenesis, Geochim. Cosmochim. Acta 43, 1075–1090, 1979.
31 R. Karlin and S. Levi, Geochemical and sedimentological control of the magnetic properties of hemipelagic sediments, J. Geophys. Res. 90, 10373–10392, 1985.
32 D.E. Canfield and R.A. Berner, Dissolution and pyritization of magnetite in anoxic marine sediments, Geochim. Cosmochim. Acta 51, 645–659, 1987.
33 D.E. Canfield, Reactive iron in marine sediments, Geochim. Cosmochim. Acta 53, 619–632, 1989.
34 B.W. Leslie, D.E. Hammond, W.M. Berelson and S.P. Lund, Diagenesis in anoxic sediments from the California continental borderland and its influence on iron, sulfur and magnetic behavior, J. Geophys. Res. 95, 4453–4470, 1990.
35 D.R. Lovley and E.J.P. Phillips, Availability of ferric iron for microbial reduction in bottom sediments of the freshwater tidal Potomac River, Appl. Environ. Microbiol. 52, 751–757, 1986.
36 D.R. Lovley, J.F. Stolz, G.L. Nord, Jr. and E.J.P. Phillips, Anaerobic production of magnetite by a dissimilatory iron-reducing microorganism, Nature 330, 252–254, 1987.

37 M. Farina, D.M.S. Esquivel and H.G.P. Lins de Barros, Magnetic iron-sulphur crystals from a magnetotactic microorganism, Nature 343, 256–258, 1990.
38 R.A. Berner, T. Baldwin and G.R. Holdren, Authigenic iron sulfides as paleosalinity indicators, J. Sediment. Petrol. 49, 1345–1350, 1979.
39 R.A. Berner, A new geochemical classification of sedimentary environments, J. Sediment. Petrol. 51, 359–365, 1981.
40 S. Wilson, J. Thomson, S. Colley, D.J. Hydes, N.C. Higgs and J. Sørensen, Early organic diagenetis: The significance of progressive subsurface oxidation fronts in pelagic sediments, Geochim. Cosmochim. Acta 49, 811–822, 1985.
41 S. Wilson, J. Thomson, D.J. Hydes, S. Colley, F. Culkin and J. Sørensen, Oxidation fronts in pelagic sediments: Diagenetic formation of metal rich layers, Science 232, 972–975, 1986.
42 G.J. de Lange, J.J. Middelburg and P.A. Pruysers, Discussion: Middle and Late Quaternary depositional sequences and cycles in the eastern Mediterranean, Sedimentology 36, 151–158, 1989.
43 P.A. Pruysers, de G.J. Lange, J.J. Middelburg and D.J. Hydes, The diagenetic formation of metal-rich layers in sapropel-containing sediments in the Eastern Mediterranean, Geochim. Cosmochim. Acta, in press, 1993.
44 W. Stumm and J.J. Morgan, Aquatic Chemistry, 780pp., Wiley, New York, 1981.
45 G.W. Luther III, Pyrite oxidation and reduction: Molecular orbital theory considerations, Geochim. Cosmochim. Acta 51, 3193–3199, 1987.
46 R. Karlin, Magnetic mineral diagenesis in suboxic sediments at Bettis Site W-N, NE Pacific Ocean, J. Geophys. Res. 95, 4421–4436, 1990.
47 D.A. Bazylinski, R.B. Frankel and H.W. Jannasch, Anaerobic magnetite production by a marine, magnetotactic bacterium, Nature 334, 518–519, 1988.
48 W.E. Dean, J.V. Gardner, and E. Hemphill-Haley, Changes in redox conditions in deep-sea sediments of the subarctic North Pacific Ocean: possible evidence for the presence of North Pacific Deep Water, Paleocanography 4, 639–653, 1989.
49 I. Jarvis and N. Higgs, Trace metal mobility during early diagenesis in distal turbidities: Late Quaternary of the Madeira abyssal plain N. Atlantic, in: Geology and Geochemistry of Abyssal Plains, P.P.E. Weaver and J. Thomson, eds., Geol. Soc. London Spec. Publ. 31, 179–215, 1987.
50 B.J.H. van Os, J.J. Middelburg and G.J. de Lange, Possible diagenetic mobilization of barium in sapropelic sediment from the eastern Mediterranean, Mar. Geol. 110, 125–136, 1991.
51 J.E.T. Channell, R. Freeman, F. Heller and W Lowrie, Timing of diagenetic haematite growth in red pelagic limestones from Gubbio (Italy), Earth Planet. Sci. Lett. 58, 189–201, 1982.
52 P.B. deMenocal, W.F. Ruddiman and D.V. Kent, Depth of post-depositional remanence acquisition in deep-sea sediments: A case study of the Brunhes-Matuyama reversal and oxygen isotope stage 19.1, Earth Planet. Sci. Lett. 99, 1–13, 1990.
53 M.J. Dekkers, Some rock magnetic parameters for natural goethite, pyrrhotite and fine-grained hematite, Geol. Ultraiectina 51, 1–230, 1988.
54 A. McIntyre, W.F. Ruddimann, K. Karlin and A.C. Mix, Surface water response of the equatorial Atlantic Ocean to orbital forcing, Paleoceanography 4, 19–55, 1989.
55 J.W. Morse and J.C. Cornwall, Acid volatile sulphides and pyrite in recent anoxic marine sediments, Mar. Chem. 22, 55–69, 1987.